Revue des Energies Renouvelables Vol. 22 N°1 (2019) 65 - 76
DOI: https://doi.org/10.54966/jreen.v22i1.726

Estimating solar radiation in a clear sky on a horizontal surface from common meteorological a data in Oran, Algeria

Fodhil Lantri [1 *] , Nour El Islam Bachari [2 †] and Ahmed Hafid Belbachir [1]

[1] Department of Physical Engineering, Faculty of Physics
University of Science and Technology Mohamed-Boudiaf, El Mnaouar,
B.P. 1505, Bir El Djir, 31000, Oran, Algeria
[2] Faculty of Biological Sciences, University of Science and Technology
U.S.T.H.B., Alger, Algeria

(reçu le 20 Février 2019 - accepté le 20 Mars 2019)

Abstract - *This study aimed to calibrate existing model (Platt and Paltridge model) and develop a new models for estimating the different components of the solar radiation on a horizontal surface in a clear sky data using commonly and available measured meteorological records such as water vapor tension and temperature, etc. Four models based on meteorological variables were generated and validated using daily data in 2013-2016 at the Oran Station (Algeria). Validation criteria included coefficient of determination, root mean square error and mean bias error, the results showed that the proposed models can estimate solar radiation values. The model based on the temperature and the water vapor tension gives better results with statistical errors obtained are as follows: NDMBE = 13.36 %, NDRMSE = 47.08 % and the correlation coefficient R = 0.85 for the diffused component, the model based on relative humidity and atmospheric pressure gives better results for the direct component with statistical errors obtained are: NDMBE = -1.54 %, NDRMSE = 22.59 % and the correlation coefficient R = 0.95 and The model based on the relative humidity and the water vapor tension with results: NDMBE = 0.96 %, NDRMSE = 12.08 % and the correlation coefficient R = 0.98 for the global component.*

Résumé - *Cette étude visait à calibrer le modèle existant (modèle de Platt et de Paltridge) et à développer de nouveaux modèles pour estimer les différentes composantes du rayonnement solaire sur une surface horizontale pour un ciel clair à l'aide de données météorologiques mesurées couramment et disponibles telles que la tension et la température de vapeur d'eau, etc. Quatre modèles basés sur des variables météorologiques ont été générés et validés à partir de données quotidiennes entre 2013-2016 à la station d'Oran (Algérie). Les critères de validation comprenaient le coefficient de détermination, l'erreur quadratique moyenne et l'erreur de biais moyenne, les résultats ont montré que les modèles proposés peuvent estimer les valeurs du rayonnement solaire. Le modèle basé sur la température et la tension de vapeur d'eau donne de meilleurs résultats avec les erreurs statistiques obtenues qui sont les suivantes: NDMBE = 13.36 %, NDRMSE = 47.08 % et le coefficient de corrélation R = 0.85 pour la composante diffuse. Le modèle basé sur l'humidité relative et la pression atmosphérique donne de bons résultats pour la composante directe avec les erreurs statistiques obtenues: NDMBE = -1.54 %, NDRMSE = 22.59 % et le coefficient de corrélation R = 0.95, tandis que le modèle basé sur l'humidité relative et la tension de vapeur d'eau avec les résultats suivants: NDMBE = 0.96 %, NDRMSE = 12.08 % et le coefficient de corrélation R = 0.98 pour la composante globale.*

Keywords: Meteorological variables - Solar radiation - Platt and Paltridge mode.

1. INTRODUCTION

Algeria is a vast country with an area of $2.3 \times 10^6 \, \mathrm{km}^2$. Since the 1930s, weather stations have been established.

* fodhil2009@yahoo.fr
† bacharinouri@gmail.com

On the other hand, the measurements of the solar radiation components are non-existent and if they exist, they have very long time gaps. Algeria wants to further develop renewable energies to Algeria wants to further develop renewable energies to benefit from strong solar insolation.

The estimation of solar radiation components in the clear sky is important to estimate the maximum distributed on the national territory. Faced with this demand and lack of data, several researchers have proposed the use of satellite imagery (Bachari, 2001) [1]; (Bouchouicha, 2016) [2]; (Rezzagui; 2017) [3].This technique presents an effective solution, but it totally depends on the presence of database of the satellite images on the one hand, and on the other hand it does not allow the estimation of the direct radiation and diffused radiation.

Therefore, It is interesting to use physical methods to estimate solar radiation by using meteorological data [4-12]. Lantri and Bachari, 2017 [13] based on the model of Platt and Paltridge in 1983 a software, SHAMS, have been developed to allow the estimation of different components of solar radiation based on meteorological data.

The proposed model is based on the following meteorological parameters: visibility (Vis), atmospheric pressure (P) and relative humidity (H). Among the constraints found was the lack of measured data. This lack of data directly translated by non-estimation of the components of the radiation. To remedy this problem we are interested in asking the following question:

Is it possible to estimate the different components of solar radiation using other meteorological parameters?

In this work we propose an adjustment of the model of Platt and Paltridge to estimate the different components of the solar radiation by proposing several variants according to the different meteorological variables.

2. EXPERIMENTAL

The model (Model1) presented below is a model based on the three meteorological variables: atmospheric pressure, relative humidity and visibility.

2.1 Calculation of irradiance due to direct radiation

The basic expression for total direct transmission has been suggested by Partridge and Platt [14]. According to them, the normal direct irradiance to medium distance Earth-Sun can be written

$$\hat{I}_n = \hat{I}_{sc} (\tau_{oz} \tau_r - \alpha_w) \tau_a \quad (1)$$

$\hat{I}_n$, Direct solar irradiance, W/m^2; $\hat{I}_{sc}$, Solar constant, W/m^2; τ_{oz}, Transmittance coefficient after absorption by ozone; α_w, Absorption of direct radiation by water vapor.

$$\alpha_w = (2.9.U_w) \,/\, \left((1 + 141.5.U_w)^{0.635} + 5.925.U_w\right) \quad (2)$$

U_w, The condensable water thickness is corrected by optical path of radiation through this layer, and is given by the following relation [cm].

$$U_w = W * m_r \quad (3)$$

W, The condensable water height, given by the following relation,

$$W = HR \times (P \,/\, 1013.15) \quad (4)$$

m_r, Relative optical path; HR, Relative humidity, %; P, Atmospheric pressure, mb; τ_r, The transmittance coefficient after molecular diffusion or Rayleigh. Davies *et al.* [15] have taken these words and presented the following relation:

$$\tau_r = 0.972 - 0.08262.m_a + 0.00933.m_a^2 - 0.00095.m_a^3 + 0.000437.m_a^4 \quad (5)$$

m_a, Air mass corrected by the pressure. The relation expressing this parameter is given by:

$$m_a = m_r \times (P / 1013.25) \quad (6)$$

τ_a, The transmittance coefficient after aerosol diffusion proposed by Mächler [16]. It is given by the following relation:

$$\tau_a = \left(0.97 - 1.265 \times (VIS)^{-0.66}\right) m_a^{0.9} \quad (7)$$

VIS, Visibilité $(5 < VIS < 180)$, km

2.2 Calculation of illumination due to diffuse radiation

Illumination due to diffuse radiation on a horizontal surface is calculated by the following relationship:

$$\hat{I}_d = \hat{I}_{dr} + \hat{I}_{da} + \hat{I}_{dm} \quad (8)$$

$\hat{I}_d$, Diffuse solar irradiance, W/m^2 ; $\hat{I}_{dr}$, Illumination due to the radiation scattered by the different molecules of air, W/m^2 ; $\hat{I}_{dm}$, Illumination due to the scattered radiation by multi-reflections earth-atmosphere, W/m^2 ; $\hat{I}_{da}$, Illumination due to the radiation diffused by the aerosols, W/m^2 ;

A.E. Leitch, P.B. Armstrong and K.H. Chu, '*Characteristics of dye adsorption by pretreated pine bark adsorbent*', International Journal of Environmental Studies, Vol. 63, N°1, pp. 59 - 66, 2006

(9)

θ_z, Zenital angle, °; ρ_g, Ground albedo; ρ'_a, Sky, or atmospheric albedo, without clouds. The latter is calculated by:

$$\rho'_a = 0.0685 + 0.17 \times (1 - \tau'_a)\ W_0 \quad (10)$$

W_0, Albedo of dispersion of the atmosphere.

τ'_a ,The transmittance coefficient after aerosol diffusion must be calculated by the air mass

$$m'_a = 1.666 \times (P / P_0)^3 \quad (11)$$

P_0, Atmospheric pressure of the level of the sea (1013 mb).

2.3 Illumination due to global radiation

In this model, the illumination due to global radiation is calculated by the following relation:

$$\hat{I} = \hat{I}_n \times \cos\theta_z + \hat{I}_d \quad (12)$$

$\hat{I}$, Global solar irradiance, W/m^2

2.4 Model reformulation technique

In this section, we will present the laws and relationships that allow us to substitute a meteorological variable with another one and generate new relationships linking the different meteorological variables to one another.

2.4.1 Behavior of the air (gas mixture).

The experiments on the air show that it behaves like a perfect gas at low pressures. That is, at low pressures, the air state variables are related to the ideal gas state equation.

The Gay-Lussac law [17] stipulates that at constant volume V, the pressure of a perfect gas is directly proportional to the absolute temperature (expressed in K), for the same quantity of gas in two state temperatures (T_0, T) and pressures (P_0, P) at the same volume:

$$(P_0 / T_0 = P / T)$$

So,

$$T = \frac{273.15 \times P}{1013} \times 25 \tag{13}$$

$$P = \frac{1013.25 \times P}{273} \times 15 \tag{14}$$

2.4.2 Relative humidity

Cloud formation usually begins as soon as the initially moist air becomes saturated with liquid water. It is conceivable then that the chances of cloud formations are even bigger as the air is close to saturation. It is then interesting to be able to estimate this proximity of the saturation. The relative humidity (hr) gives us this information: hr = (P_w / P_s(t)).

The relative humidity is usually given as a percentage and is represented by HR [18]:

$$HR = 100 \times hr = 100 \times (P_w / P_s(T)) \tag{15}$$

P_W = Water vapor tension (partial pressure of the water vapor) [hPa]

P_S (T) = Saturated water vapor tension at T given according to the temperature by [hPa]:

$$P_s(T) = 6.1078 \times \exp\left(17.269 \times \frac{T}{237.3 + T}\right) \tag{16}$$

2.4.3 The new relationships

2.4.3.1 Relative humidity as a function of the temperature and the water vapor tension

From equations (15) and (16) we have:

$$HR = 16.3725 \times P_w \times \left(\exp\left(17.269 \times \frac{T}{237.3 + T}\right)\right)^{-1}$$

After simplification we find:

$$HR = 5.18 \times 10^{-7} \times P_w \times \exp\left(4097 \times \frac{9337}{237.3 + T}\right) \tag{17}$$

3.1.3.2 Relative humidity as a function of the pressure and the water vapor tension

From equations (15) and (16) we have:

$$HR = 5.18 \times 10^{-7} \times P_w \times \exp\left(4097 \times \frac{9337}{237.3 + \left(273.15 \times \left(P/1013 \right).25 \right)} \right)$$

After simplification we find:

$$HR = 5.18 \times 10^{-7} \times P_w \times \exp\left(15201 \times \frac{2862}{880.2644 + P} \right) \quad (18)$$

2.4.3.3 Temperature as a function of the relative humidity and the water vapor tension

From equation (17) we have:

$$\text{Exp}\left(4097 \times \frac{9337}{237.3 + T} \right) = \frac{HR}{5.18 \times 10^{-7} \times P_w}$$

After simplification we find:

$$T = 4097.9337 \times \left(\ln\left(\frac{HR}{5.18 \times 10^{-7} \times P_w} \right) \right)^{-1} - 237.3 \quad (19)$$

2.4.3.4 Pressure as a function of the relative humidity and the water vapor tension

From equations (19) and (13) we have:

$$\frac{273.15 \times P}{1013}.25 = 4097.9337 \times \left(\ln\left(\frac{HR}{5.18 \times 10^{-7} \times P_w} \right) \right)^{-1} - 237.3$$

After simplification we find:

$$P = 15201.2862 \times \left(\ln\left(\frac{HR}{5.18 \times 10^{-7} \times P_w} \right) \right)^{-1} - 880.2644 \quad (20)$$

2.5 New Models

As we saw earlier, the initial model is based on atmospheric pressure, relative humidity and visibility; we substitute one or two meteorological variables each time with new ones, with the exception of visibility. And the relations concerned with the substitution are:

The condensable water height

$$W = HR.\left(\frac{P}{1013} . 25 \right) \quad (21)$$

Air mass corrected by pressure

$$m_a = m_r . \left(\frac{P}{1013}.25 \right) \quad (22)$$

Air mass

$$m'_a = 1.666 \times \left(P / P_0 \right)^3 \quad (23)$$

2.51 Model 2 (based on velocity, relative humidity and temperature

For {Eq. (14)} and {Eq. (4)}, we have

$$W = HR.\left(\frac{T}{273.15}\right) \tag{24}$$

For {Eq. (14)} and {Eq. (6)}, we have

$$m_a = m_r \cdot \left(\frac{T}{273.15}\right) \tag{25}$$

For {Eq. (14)} and {Eq. (11)}, we have

$$m'_a = 1.666 \times \left(\frac{T}{273.15}\right)^3 \tag{26}$$

2.52 Model 3 (based on velocity, relative humidity and water vapor pressure)

For {Eq. (20)} and {Eq. (4)}, we have

$$W = HR.\left(15\times\left(\ln\left(\frac{HR}{(5.18\times10^{-7}\times P_W)}\right)\right)^{-1} - 0.8687\right) \tag{27}$$

For {Eq. (20)} and {Eq. (6)}, we have

$$m_a = m_r \cdot \left(15\times\left(\ln\left(\frac{HR}{(5.18\times10^{-7}\times P_W)}\right)\right)^{-1} - 0.8687\right) \tag{28}$$

For {Eq. (20)} and {Eq. (11)}, we have

$$m'_a = 1.666 \cdot \left(15\times\left(\ln\left(\frac{HR}{(5.18\times10^{-7}\times P_W)}\right)\right)^{-1} - 0.8687\right)^3 \tag{29}$$

2.53 Model 4 (based on visibility, water vapor pressure and temperature)

For {Eq. (17)} and {Eq. (4)}, we have

$$W = 18.967\times10^{-10}\times T\times P_w\times\exp\left(\frac{4097.9337}{237.3+T}\right) \tag{30}$$

m_a and m'_a are given by {Eq. (22)} and {Eq. (23)} respectively.

2.54 Model 5 (based on visibility, water vapor pressure and pressure)

For {Eq. (18)} and {Eq. (4)}, we have

$$W = 5.1123\times10^{-10}\times P\times P_w\times\exp\left(\frac{15201.2862}{(880.2644+P)}\right) \tag{31}$$

m_a and m'_a are given by {Eq. (6)} and {Eq. (11)} respectively.

2.6 Statistical Formulas

2.6.1 Statistical errors

Widely used statistical errors [19] are biased mean error (MBE) and mean squared error (RMSE).

Percentage deviations or a fraction of the estimated value from the measured value and the mean relative error (MERR) defined as follows:

2.6.1.1 Average error

$$MBE = \left(\sum_1^n (H_{ci} - H_{mi}) \right) \Big/ n \tag{32}$$

or in percentage

$$NDMBE = \left(\left(\left(\sum_1^n (H_{ci} - H_{mi}) \right) / n \right) \right) \times \left(100 / \overline{H}_m \right) \tag{33}$$

The mean error (MBE or NDMBE) gives an indication of an underestimate or an overestimate [20] of the model in relation to the measures; it is negative if the model is underestimated, conversely, if it is overestimated.

2.6.1.2 Mean quadratic error

$$RMSE = \left(\left(\sum_1^n \left(H_{ci} - H_{mi} \right) \right)^2 \Big/ n \right)^{1/2} \tag{34}$$

or in percentage

$$NDRMSE = \left(\left(\sum_1^n \left(H_{ci} - H_{mi} \right) \right)^2 \Big/ n \right)^{1/2} \times \left(100 / \overline{H}_m \right) \tag{35}$$

Root mean squared error (RMSE or NDRMSE) represents the reliability of the models. RMSE is even smaller as the model gets closer to the measurement results.

2.6.2 Coefficient of correlation (R)

The Correlation coefficient [21] can be used to determine the linear relationship between measured values and estimated values, which can be calculated by the following equation

$$R = \frac{\sum_1^n (H_{ci} - H_c) \times (H_{mi} - \overline{H}_m)}{\left(\sum_1^n (H_{ci} - H_c)^2 \times \sum_1^n (H_{mi} - \overline{H}_m)^2 \right)^{1/2}} \tag{36}$$

The indicator varies between -1 and 1. A value of 1 or close to 1 indicates a perfect agreement between the measured and calculated value. A value of -1 or close to -1 indicates a perfect inverse relationship between the measured and calculated value. On the other hand, a value close to 0 indicates a total disagreement.

3. RESULTS AND DISCUSSION

3.1 The data used

The data used in this work relate to an Algerian site, Oran. Thus, the geographical characteristics of this site are given in the following table:

Table 1: Geographical features of Oran site

Site	Latitude (°)	Longitude (°)	Altitude (m)	Period of comparison
ORAN	35.63	0.6	90	2013-2014-2015-2016

3.2 The seasonal scale

Table 2: Statistical errors of different components for each season of the year.

Components	Models	Errors	Winter	Spring	Summer	Autumn
global	Model 1	NDRMSE (%)	**21,63**	5,59	9,55	16,54
		NDMBE (%)	**-4,83**	1,34	6,52	4,55
	Model 2	NDRMSE (%)	21,78	**5,58**	8,57	16,31
		NDMBE (%)	-5,44	0,34	5,14	3,65
	Model 3	NDRMSE (%)	21,77	5,61	**8,2**	**16,3**
		NDMBE (%)	-5,41	**0,08**	4,56	3,51
	Model4	NDRMSE (%)	24,28	10,52	8,95	16,75
		NDMBE (%)	-10,98	-7,24	**-3,9**	**-3,46**
	Model 5	NDRMSE (%)	42,45	50,85	35,34	61,74
		NDMBE (%)	17,54	28	-4,81	37,78
direct	Model 1	NDRMSE (%)	27,3	17,6	23,03	23,4
		NDMBE (%)	-9,51	-6,57	10,72	**-2,93**
	Model 2	NDRMSE (%)	28,07	19,63	21,36	24,1
		NDMBE (%)	-11,03	-9,6	6,03	-5,18
	Model 3	NDRMSE (%)	28,05	20,22	**20,97**	24,3
		NDMBE (%)	-10,97	-10,37	4,11	-5,54
	Model4	NDRMSE (%)	31,81	25,33	21,63	27,59
		NDMBE (%)	-16,5	-16,72	**-3,51**	-12,01
	Model 5	NDRMSE (%)	**24,86**	**15,38**	27,26	**23,36**
		NDMBE (%)	**-2,21**	**0,15**	17,66	4,42
diffuse	Model 1	NDRMSE (%)	43,82	53,3	35,85	64,18
		NDMBE (%)	19,35	30,72	-3,38	40,44
	Model 2	NDRMSE (%)	47,52	58,73	36,32	69,22
		NDMBE (%)	23,39	37,24	3,01	46,11
	Model 3	NDRMSE (%)	47,61	60,23	36,88	70,15
		NDMBE (%)	23,31	38,92	5,62	47,13
	Model 4	NDRMSE (%)	**42,45**	**50,85**	**35,34**	**61,74**
		NDMBE (%)	**17,54**	**28**	-4,81	**37,78**
	Model 5	NDRMSE (%)	50,21	60,3	36,79	72,22
		NDMBE (%)	26,61	38,63	**1,77**	48,92

Table 2 shows the statistical results obtained from all models for each season of the year, through the table, we observe the following

3.2.1 Winter- We find that all models underestimate the measurements of both components (direct and global), except in the case of model 5 in the global component that overestimate the measurements of the diffuse component.

We note that the lowest quadratic error value corresponds to model1 for the global component, model 5 for the direct component and model 4 for the diffuse. The NDRMSE values are equal to 21.63 %, 24.86 % and 42.45 % respectively.

3.2.2 Spring- We find that all the selected models overestimate the measures for both components (diffuse and global), except in the case of model 4 of the global component that underestimate the measures for the direct component; and in the case of model 5 that overestimates the measurements of the diffuse component.

We note that the lowest quadratic error value corresponds to model 2 for the global component, model 5 for the direct component and model 4 for the diffuse. The NDRMSE is equal to 5.58 %, 15.38 % and 50.85 % respectively.

3.2.3 Summer- We note that model 4 underestimates the measurements of the three components, models 1 and 5 respectively underestimate the measurements in the diffuse and global components and models 2 and 3 overestimate the measurements of the three components.

In the case of a direct component, the mean squared error (NDRMSE) is smaller for model 3; and this value is equal to 20.97 %.

In the case of a diffuse component, (NDRMSE) is lower for model 4 and its value is equal to 35.34 %. As for the global component, model 3 has a value of (NDRMSE) equal to 8.2 %.

3.2.4 Autumn- We find that all the chosen models overestimate the measures for both components (diffuse and global), except for model 4 in the global component that underestimate the measures for the direct component; and for model 5.

In the case of a direct component, the mean squared error (NDRMSE) is lower for model 5, and this value is equal to 23.36 %. In the case of a diffuse component, (NDRMSE) is lower for model 4 and its value is equal to 61.74 %; and for the global component, model 3 is with a value of (NDRMSE) equal to 16.3 %.

We can note that the best estimates for the global and direct components relate to spring and summer; and in the case of diffuse component the best estimates in winter and summer.

3.3 The annual scale

Table 3: Coefficient of correlation R between the measured and calculated values for three components of solar radiation for each mode

Component	Model 1	Model 2	Model 3	Model 4	Model 5
Global	0,98	0,98	0,98	0,98	0,98
Direct	0,95	0,95	0,95	0,95	0,95
Diffuse	0,85	0,86	0,86	0,85	0,85

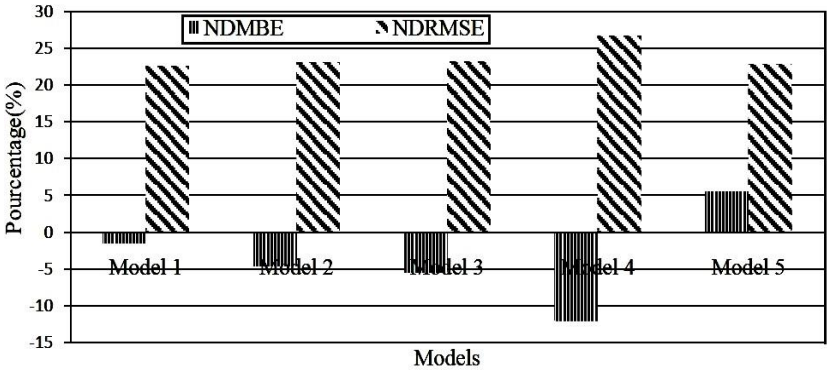

Fig. 1: Errors NDMBE and NDRMSE of daily solar radiation for each mode (direct component)

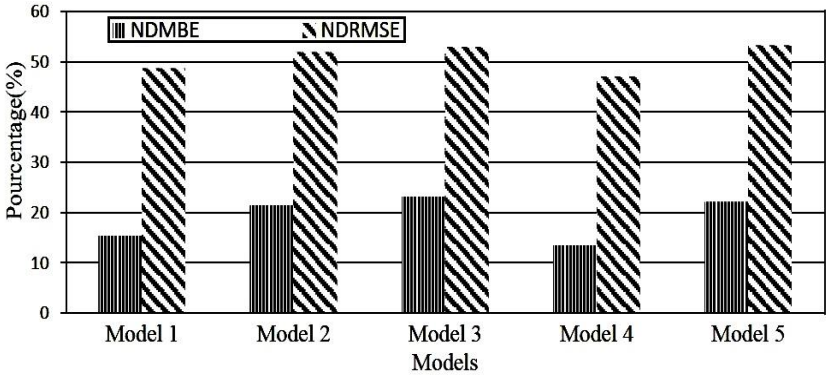

Fig. 2: Errors NDMBE and NDRMSE of daily solar radiation for each mode (diffuse component)

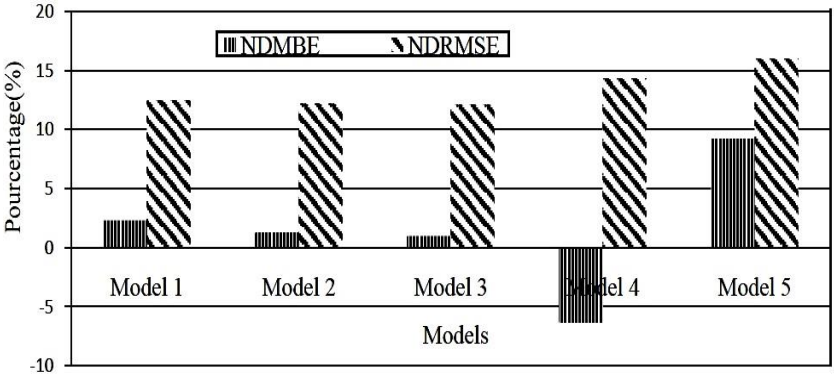

Fig. 3: Errors NDMBE and NDRMSE of daily solar radiation for each mode (global component)

Figure 1, figure 2 and figure 3 illustrate the statistical errors of different components of daily solar radiation for each mode, through these figures, we observe the following.

3.3.1 Direct- We find that all the selected models underestimate the measures, except in the case of the model 5 where the measures are overestimated. We note that the lowest quadratic error value corresponds to model 1. The NDRMSE is equal to 22.59 %.

3.3.2 Diffuse- We find that all the models overestimate the measurements. We note that the lowest quadratic error value corresponds to model 4. The NDRMSE is equal to 47.08 %

3.3.3 Global- We find that all the selected models overestimate the measures, except in the case of model 4. We note that the lowest squared error value corresponds to model 3 and is equal to 12.08 %.

Table 3 shows that there is a strong correlation between the measured and calculated values of the global and direct components and a lower value for the diffuse component for all models.

4. CONCLUSION

In the absence of radiation data, reliable estimates can be made from easily available meteorological observations of temperature, relative humidity etc....

In this study, using the Oran station (Algeria) as a case study, one model exist and Four proposed models were calibrated and evaluated using the daily meteorological data from January 2013 to December 2016 for estimating the different components of the solar radiation on a horizontal surface in a clear sky.

From the previous study we propose a strategy for selecting an optimal method, for estimating daily components of solar radiation in Oran: for estimated the direct component, we use Model 1 (based on relative humidity and atmospheric pressure); when to estimated the diffused component, we use Model 4 (based on the temperature and the water vapor tension) and use Model 3 (based on the relative humidity and the water vapor tension) for estimated the global component.

Through all of the above we conclude, that in the case of gaps in measurements of a meteorological variable can be calculated or replace with other meteorological variables with ease, but the performance of the new variables varies according to the seasons of the year as well as the component to be estimated.

REFERENCES

[1] N.E.I. Bachari et A. Razagui, '*Estimation et Cartographie des Différentes Composantes du Rayonnement Solaire à Partir des Images Météosat*', Revue des Energies Renouvelables, Vol. 4, pp. 35 - 47, 2001.

[2] K. Bouchouicha, A. Razagui, N.E.I Bachari and N. Aoun, '*Hourly global solar radiation estimation from MSG-SEVIRI images-case study: Algeria*', World Journal of Engineering, Vol. 13, N° 3, pp. 266 - 274, 2016.

[3] A. Razagui, N.E.I. Bachari, K. Bouchouicha and A. Hadj Arab, '*Modeling the Global Solar Radiation Under Cloudy Sky Using Meteosat Second Generation High Resolution Visible Raw Data*', Journal of the Indian Society of Remote Sensing, ISSN 0255-660X, 2017.

[4] M. Mesri, A. Cheknane, N.E.I. Bachari and I. Rougab, '*Estimation of monthly total radiation daily by two weather approach in Algeria*', Canadian Journal of Physics Vol. 89, N°12, pp. 1215 -1218, 2011, ISSN: 1208-6045.

[5] M. El-Metwally, '*Sunshine and global solar radiation estimation at different sites in Egypt*', Journal of Atmospheric and Solar-Terrestrial Physics, Vol. 67, N°14, pp. 1331 - 1342, 2005.

[6] A. Yag, '*New correlation of global solar radiation with meteorological parameters for Bahrain*', International Journal of Solar Energy, Vol. 16, pp. 111 - 120, 1994.

[7] M.G. Abraha and M.J. Savage, '*Comparison of estimates of daily solar radiation from air temperature range for application in crop simulations*', Agricultural and Forest Meteorology, Vol. 148, N°3, pp. 401 - 416, 2008.

[8] L.E. Akpabio, S.O. Udo and S.E. Etuk, '*Empirical correlation of global solar radiation with Meteorological data for Onne, Nigeria*', Turkish Journal of Physics, Vol. 28, N°3, pp. 222 - 227, 2004.

[9] J. Almorox, C. Hontoria and M. Benito, '*Models for obtaining daily global solar radiation with measured air temperature data in Madrid (Spain)*', Applied Energy, Vol. 88, pp. 1703 - 1709, 2011.

[10] K. Bakirci, '*Models of solar radiation with hours of bright sunshine*', Renewable and Sustainable Energy Reviews Vol.13, p 2580-2588, 2009.

[11] M.A. Behrang, E. Assareh, A. Ghanbarzadeh and A.R. Noghrehabadi, '*The potential of different artificial neural network (ANN) techniques in daily global solar radiation modelling based on meteorological data*', Solar Energy, Vol. 84, pp. 1468 - 1480, 2010.

[12] J.L. Chen, H.B. Liu, W. Wu and D.T. Xie, '*Estimation of monthly solar radiation from measured temperatures using support vector machines*', Renewable Energy, Vol. 36, pp. 413 - 420, 2011.

[13] F. Lantri, N.E.I. Bachari et H. Belbachir, '*Estimation et Cartographie des différentes composantes de rayonnement solaire au Sol à Partir des données météorologiques*', Revue des Energies Renouvelables Vol. 20 N°1 pp. 111 - 130, 2017.

[14] M. Koussa, A. Malek and M. Haddadi, '*Validation de quelques modèles de reconstitution des éclairements dus au rayonnement solaire direct, diffus et global par ciel clair*', Revue des Energies Renouvelables, Vol. 9 N°4, pp. 307 - 332, 2006.

[15] D. Saheb-Koussa, M. Koussa et M. Belhamel,(2006) '*Reconstitution du Rayonnement Solaire par ciel clair*', Revue des Energies Renouvelables Vol. 9 N°2 pp 91 – 97, 2006.

[16] M. Mesri-Merad, I. Rougab, A. Cheknane et N.I. Bachari, 'Estimation du rayonnement solaire au sol par des modèles semi-empiriques', Revue des Energies Renouvelables Vol. 15 N°3 pp. 451 - 463 2012.

[17] Martha M. Day, Matthew Ignash, Lee Ann Smith, '*Learning Cycle and the Gas Laws: Constructing and Experimenting with a Ping Pong Poppe*', Journal of Laboratory Chemical Education, Vol. 1, N°4, pp. 65 - 69, 2013

[18] R. Seager, A. Hooks, A. Park Williams, B. Cook, J. Nakamura and N. Henderson, '*Climatology, Variability, and Trends in the U.S. Vapor Pressure Deficit, an Important Fire-Related Meteorological Quantity*', Journal of applied meteorology and climatology, Vol. 54, pp.1121 - 1141, 2015.

[19] S. Benkaciali et K. Gairaa, '*Techniques de modélisation de l'irradiation solaire sur un plan incliné*', International Journal of Scientific Research& Engineering Technology (IJSET) Vol. 3, pp.102 - 108, 2014.

[20] K. Kerkouche, F. Cherfa, A. Hadj Arab, S. Bouchakour, K. Abdeladim et K. Bergheul, '*Evaluation de l'irradiation solaire globale sur une surface inclinée selon différents modèles pour le site de Bouzaréah*', Revue des Energies Renouvelables, Vol. 16 N°2, pp. 269 – 284, 2013.

[21] Abdul Majeed Muzathik, Wan Mohd Norsani Wan Nik, Khalid Samo, Mohd. Zamri Ibrahim, '*Hourly Global Solar Radiation Estimates on a Horizontal Plane*'; Journal of Physical Science, Vol. 21, N°2, pp. 51 - 66, 2010